

# Mechanistic model of electrocoagulation process for treating vinasse waste: Effect of initial pH

*by Iqbal Syaichurrozi*

---

**Submission date:** 05-Apr-2023 07:13AM (UTC+0700)

**Submission ID:** 2056091598

**File name:** tion\_process\_for\_treating\_vinasse\_waste\_Effect\_of\_initial\_pH.pdf (1.22M)

**Word count:** 10673

**Character count:** 50122



Contents lists available at ScienceDirect

Journal of Environmental Chemical Engineering

journal homepage: [www.elsevier.com/locate/jece](http://www.elsevier.com/locate/jece)



## Mechanistic model of electrocoagulation process for treating vinasse waste: Effect of initial pH

Iqbal Syaichurrozi<sup>a,b</sup>, Sarto Sarto<sup>a,\*</sup>, Wahyudi Budi Sediawan<sup>a</sup>, Muslikhin Hidayat<sup>a</sup>

<sup>a</sup>Department of Chemical Engineering, Faculty of Engineering, Universitas Gadjah Mada, Jl. Grafika No.2, Yogyakarta, 55281, Indonesia

<sup>b</sup>Department of Chemical Engineering, Faculty of Engineering, University of Sultan Ageng Tirtayasa, Jl. Jendral Soedirman Km 3, Cilegon, 42435, Indonesia

### ARTICLE INFO

#### Keywords:

Electrocoagulation  
Initial pH  
Mechanistic model  
Vinasse  
Waste

### ABSTRACT

Electrocoagulation (EC) is widely applied to treat wastewaters. Vinasse is a bioethanol waste containing high Chemical Oxygen Demand (COD) and having low power Hydrogen (pH) level. Application of EC for treating vinasse has been studied by other authors, but development of mechanistic models has not been conducted yet. Because of the complex reactions in EC, building a mechanistic model is very interesting. The effect of initial pH in EC on COD removal of the vinasse was investigated and then the measured data was modeled. In the model, reactions in EC process consisted of adsorption, flocculation, entrapment, sedimentation and flotation. Measured data obtained through experiment included COD, total dissolved Fe, scum and sludge per real time during EC process. Increase in initial pH from 4.35 to 6.00 increased the kinetic constants of  $k_1$  (adsorption),  $k_e$  (entrapment) and  $k_{sc}$  (flotation). Furthermore, some mathematical equations between the initial pH and the kinetic constants were successfully founded so that the EC performance for other initial pH (in range of 4.35–6.00) could be predicted. Meanwhile, ratio between removed COD to total operating cost for initial pH of 4.35, 5.00 and 6.00 after EC process for 60 min was 0.0570, 0.0506 and 0.0636 g-COD IDR<sup>-1</sup> respectively.

### 1. Introduction

At the moment, bioethanol production in Indonesia is as much as 450 million liter per year [1]. Because the government has a target to replace fossil fuels need from 8 % (the year of 2013) to 31 % (the year of 2050) with renewable energy [2], the bioethanol production will increase significantly in the future. Unfortunately, to produce 1 L bioethanol, the industries generate 8–15 L vinasse waste [3]. The waste is a bottom product of distillation unit. It has very acidic level (pH of 3.75–4.5, [4,5]), contains high organic compound (Chemical Oxygen Demand (COD) more than 100,000 mg L<sup>-1</sup>, [3,6]) and has high COD to Nitrogen (COD/N) ratio (approximately 205 [3]). According to Budiyo et al. [7], vinasse has to be treated to decrease the COD content before it is discharged to the water bodies. Nowadays, many methods can be utilized to decrease pollutants in wastewaters such as biological, physical, chemical and physicochemical treatments.

In biological treatments, Sepehri and Sarrafzadeh [8] proposed a nitrifying-enriched activated sludge (NAS) to improve filterability in membrane bioreactors in term of removing pollutants in synthetic wastewater. This concept was effective to be applied to wastewaters having low ratio of carbon to nitrogen (C/N). At low C/N ratio, nitrifying bacteria grew well which was 10 times more than that at high

C/N ratio. It resulted high nitrification efficiency. Furthermore, Sepehri et al. [9] proposed collaboration between *Chlorella vulgaris* and NAS to remove pollutants in wastewaters. It increased nutrient removal and dissolved carbon capture. However, it was effective to be applied at low COD/N ratio because the growth rate of algae decreased at high COD/N ratio. Because vinasse contains high COD/N ratio (or C/N), the methods of NAS or algae-NAS are not suitable to be applied to treat the vinasse. In addition, the very high COD concentration, the biological treatment was not effective.

In chemical treatments, the catalytic degradation can be utilized to decrease pollutant concentration in wastewaters. Some metal and metal oxide nanoparticles (silver, platinum, gold, palladium, bimetallic composites) can be applied as nano-catalyst. However, in solution, they have a tendency to aggregate because of interparticle interactions via van der Waals forces and high surface energies [10]. That phenomenon will decrease the catalytic efficiency and stability. Hence, other components are needed to support the nanoparticles [10]. Zeng et al. [11] has successfully fabricated the novel MoS<sub>2</sub>-PDA-Ag nanocomposites via mussel-inspired chemistry and then applied them as heterogeneous catalyst to remove 4-nitrophenol through microwave irradiation. However, catalytic degradation method is not more effective than adsorption method. The latter has easier operation and lower cost [12].

16

\* Corresponding author.

E-mail address: [sarto@ugm.ac.id](mailto:sarto@ugm.ac.id) (S. Sarto).

<https://doi.org/10.1016/j.jece.2020.103756>

Received 29 October 2019; Received in revised form 2 February 2020; Accepted 5 February 2020

Available online 06 February 2020

2213-3437 / © 2020 Published by Elsevier Ltd.

Nomenclatures	
$[Fe^{2+}]$	Concentration of $Fe^{2+}$ ( $g L^{-1}$ )
$[COD]$	Concentration of COD ( $g L^{-1}$ )
$[Scum]$	Concentration of scum ( $g L^{-1}$ )
$[Sludge]$	Concentration of sludge ( $g L^{-1}$ )
$[A]$	Concentration of small aggregate ( $g L^{-1}$ )
$[A_2]$	Concentration of big aggregate ( $g L^{-1}$ )
$d$	Distance of electrodes (cm)
$e^-$	Electron
$I$	Current (Ampere)
$J$	Current density (Ampere $cm^{-2}$ )
$A_s$	Active surface of electrode ( $cm^2$ )
$t$	Electrolysis time (sec)
$v$	Volume of wastewater (L)
$M_w$	Molar mass of Fe ( $56 g mol^{-1}$ )
$z$	Number of electron transfer (2 or 3)
$F$	Faraday's constant ( $96,500 C mol^{-1}$ )
$k_1$	Reaction rate constant for adsorption ( $L g^{-1} sec^{-1}$ )
$k_2$	Reaction rate constant for flocculation ( $L g^{-1} sec^{-1}$ )
$k_a$	Reaction rate constant for oxidation at anode ( $sec^{-1}$ )
$k_c$	Reaction rate constant for reduction at cathode ( $sec^{-1}$ )
$k_e$	Reaction rate constant for entrapment ( $sec^{-1}$ )
$k_{sc}$	Reaction rate constant for flotation ( $sec^{-1}$ )
$k_{sd}$	Reaction rate constant for sedimentation ( $sec^{-1}$ )
$EnC$	Energy consumption ( $Ws L^{-1}$ )
$ELC$	Electrode consumption ( $g L^{-1}$ )
$ChC$	Chemical consumption ( $kg L^{-1}$ )
$V$	Voltage (Volt)
$\kappa$	Conductivity ( $\mu S cm^{-1}$ )

In physical treatments, some authors found that modified materials, as adsorbent, are effective to adsorb the specific pollutants. The mussel-inspired chemistry has been widely utilized for the fabrication of functional composites for catalytic degradation [10], environmental adsorption [10] and drug delivery application [2, 3]. The mussel adhesive protein in mussel mucus corresponds to the strong adhesion of the mussel. The key component of it is the 3,4-dihydroxy-L-phenylalanine (DOPA). Furthermore, dopamine (DA) is one of DOPA derivative and polydopamine (PDA) is self-polymerization of DA [10]. The PDA nanoparticles could be used as an adsorbent for Copper (II) ( $Cu^{2+}$ ) [12]. To increase an adsorption capacity, the PDA and DOPA with other components are used to make the novel composites that are used as adsorbents. The polyacrylamide immobilized molybdenum disulfide ( $MoS_2@PDA@PAM$  composites) [14], the carbon nanotubes based carboxymethyl chitosan nanocomposites (CNT-PDA-CS nanocomposites) [15], the functionalized carbon nanotubes with polydopamine and polyethylene polyamine (CNTs-PDA-PP) [16] showed satisfied results in  $Cu^{2+}$  removal by adsorption method. Furthermore, the functionalized  $SiO_2$  nanoparticles with cationic polymers poly((3-Acrylamidopropyl)trimethylammonium chloride) ( $SiO_2$ -PDA-PAPTCl) [17] and the functionalized Molybdenum disulfide with self-polymerization of levodopa ( $MoS_2$ -PDOPA polymer) [14] could remove organic dye. The other materials such as the polyethylene polyamine@tannic acid encapsulated MgAl-layered double hydroxide (LDH-PP@TA) [19],

the polyacrylamide immobilized molybdenum disulfide ( $GO-Fe_3O_4$  composites) [20] and the polyethylenimine-tannins coated  $SiO_2$  ( $SiO_2@PEI-TA$ ) hybrid materials [21] also could adsorb  $Cu^{2+}$ . Meanwhile, the functionalized carbon nanotubes with tannins (CNT-TA) [22] and the sulfonic groups functionalized Mxenes ( $Ti_3C_2-SO_3H$ ) [23] could remove methylene blue. Adsorption is effective for low pollutant concentration not for high pollutant concentration because it needs so many adsorbents for high pollutant concentration.

In physicochemical treatment, one of potential methods to treat vinasse is electrocoagulation (EC). Many authors reported that the COD in vinasse was successfully decreased through EC [24–29]. Application of EC for treating wastewaters is very attracting because of its advantages i.e simple equipment, easy operation, rapid sedimentation rate, low capital and operating cost, shortened retention period and very efficient in COD removal [30–34]. The main process for COD removal in EC is adsorption by coagulants of  $Fe(OH)_2$  and  $Fe(OH)_3$ . The EC may be more efficient than adsorption by using adsorbents (previous paragraph), because the coagulants (such as  $Fe(OH)_2$  and  $Fe(OH)_3$ ) are continuously produced due to electrical force during EC process. EC uses metals as electrodes. Anode and cathode are electrodes connected to positive and negative poles of power Direct Current (DC) supply. The electrodes are immersed in wastewaters. Iron (Fe) is a common metal used as electrode in this method. Meanwhile, contaminant removal efficiency was obtained higher by using Fe electrode

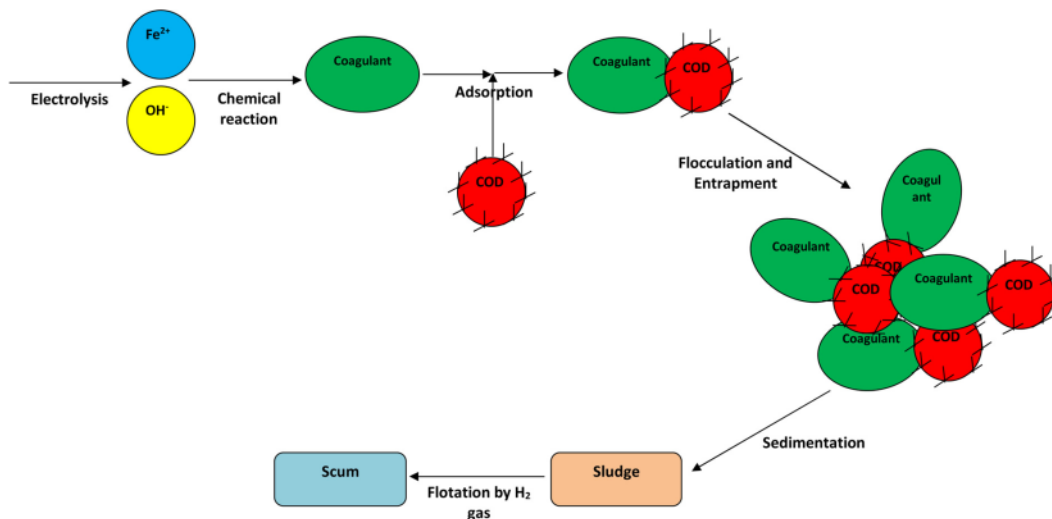


Fig. 1. Mechanism process during EC.

than by using Al electrode [35,36]. When a current is flowing, sacrificial anode (Fe) is dissolved to be  $Fe^{2+}$  ion. Meanwhile, the  $H_2O$  is to be  $H_2$  and  $OH^-$  ion. Furthermore,  $Fe^{2+}$  is hydrolyzed to be coagulant of  $Fe(OH)_2$  and  $Fe(OH)_3$ . The coagulants will adsorb the pollutants, hence favoring the formation of aggregates. The aggregates react each other to make the bigger aggregate via flocculation. The aggregates can be removed by sedimentation as sludge and by flotation as scum by evolved  $H_2$  [37,38].

Degradation of pollutants during EC can be modeled by using adsorption kinetic models (empirical models) such as pseudo first order model, pseudo second order model, Langmuir model, Elovich model and fractional power model [39,40]. These models are used with assuming that the adsorption is limiting step in EC. However, it is very interesting to see the complex mechanism processes during EC. Thus, a mechanistic model has to be built to describe step by step of reactions in EC process. Based on our study of literatures, however, at the moment, there is no mechanistic model for EC, especially in term of vinasse treatment. Hence, this study proposed a novel mechanistic model that is new and original. For kinetic analysis using the mechanistic model, the experimental data was obtained from EC of vinasse at variation of initial pH.

Initial pH is one of the most factors affecting the pollutant removal. It is more important than current density [41]. According to Demirbas and Kobya [30], by using Fe electrode, initial pH of 6–7 resulted the more COD removal efficiency than the others with range of 3–8. Furthermore, Olya and Pirkarami [42] reported that the optimum initial pH in organic contaminant removal by using Fe-Fe electrode was 6. In this study, vinasse has low pH level (pH of 4.35, see point of 4.1). Therefore, this study varied the initial pH of vinasse to be 4.35, 5.00 and 6.00 by using NaOH. The neutral condition (pH of 7) was not conducted because it might result the almost same COD removal efficiency with pH of 6. Alkaline condition (pH of 8–14) was not conducted because it needs much more NaOH addition but the COD removal is low.

The mechanistic model contains some kinetic constants presenting the phenomena during EC process. For fitting between measured and predicted data, the kinetic constants have to be searched until the fitting error value is low. Furthermore, the mathematical correlation between the initial pH (4.35, 5.00, 6.00) and the kinetic constants would be built, so that the EC performance for other initial pH with range 4.35–6.00 could be predicted.

## 2. Mechanism of EC process

As illustration, Fig. 1 shows the mechanisms during EC. In this study, all processes are assumed to be irreversible process. Furthermore, decrease in wastewater volume during EC is ignored, so the volume is assumed to be constant. When iron is used as sacrificial anode in EC,  $Fe^{2+}$  ion is dissolved in the wastewater by the oxidation reaction at the anode (Eq. (1), [37]).



Meanwhile,  $OH^-$  ion and  $H_2$  gas are resulted by water reduction reaction at the cathode (Eq. (2), [37]).



Accumulation of  $OH^-$  ion increases the solution pH. Because of the pH level,  $Fe^{2+}$  ion is hydrolyzed to be insoluble coagulants of  $Fe(OH)_2$  (Eq. 3a). It also can be oxidized to be  $Fe^{3+}$  and then hydrolyzed to be  $Fe(OH)_3$  [43]. Besides that, the  $Fe^{2+}$  and  $Fe^{3+}$  is also hydrolyzed to be  $Fe(OH)^+$ ,  $Fe(OH)_2^+$  and  $Fe(OH)_2^+$  that can be acting as coagulant too but they presents poor coagulative activity [37].



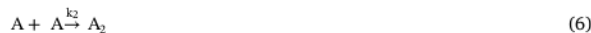
The coagulants adsorb the pollutants (COD) to make small aggregate as shown in Eq. (4).



Because of spontaneous oxidation and hydrolysis of  $Fe^{2+}$  to be the coagulants, the rate-determining step is generation ion  $Fe^{2+}$  electrolytically [44]. Eq. (4) could be rewritten to be:



After that, the flocculation occurs when the small aggregate (A) reacts each other to make the big aggregates (Eq. (6)).



In  $A_2$  formation, the pollutant (COD) might be entrapped in it (Eq. (7)).



The aggregates can be separated by sedimentation as sludge on the base (Eq. (8)). However, a part of sludge can go up as scum due to flotation by evolved  $H_2$  during EC process (Eq. (9)).



Therefore, the mechanism of EC could be summarized in Table 1.

## 3. Modeling

### 3.1. Net rate of $Fe^{2+}$ production

Rate of  $Fe^{2+}$  ion production per second time by anode oxidation can be predicted through Faraday's law [44,45].

$$\frac{d[Fe^{2+}]}{dt} = \frac{IM_w}{zFv} \quad (10)$$

Since  $I$  is  $JA_s$ , Eq. (10) is modified to be Eq. (11)

$$\frac{d[Fe^{2+}]}{dt} = \frac{JM_wA_s}{zFv} \quad (11)$$

Rate of  $Fe^{2+}$  ion consumption for adsorbing COD is expressed by:

$$\frac{d[Fe^{2+}]}{dt} = -k_1[Fe^{2+}][COD]$$

Hence, the net rate of  $Fe^{2+}$  production is shown in Eq. (12).

$$\frac{d[Fe^{2+}]}{dt} = \frac{JM_wA_s}{zFv} - k_1[Fe^{2+}][COD] \quad (12)$$

### 3.2. Net rate of A production

Rate of A production from adsorption of COD on coagulant is

**Table 1**  
The step by step of EC mechanism.

Reaction	Description
$Fe^{2+} + \text{COD} \xrightarrow{k_3} A$	Adsorption
$A + A \xrightarrow{k_4} A_2$	Flocculation
$\text{COD} \xrightarrow{k_5} A_2$	Entrapment
$A_2 \xrightarrow{k_6} \text{Sludge}$	Sedimentation
$\text{Sludge} \xrightarrow{k_7} \text{Scum}$	Flotation



expressed by:

$$\frac{d[A]}{dt} = k_1 [Fe^{2+}][COD]$$

Rate of A consumption for producing  $A_2$  is expressed by:

$$\frac{d[A]}{dt} = -k_2 [A]^2$$

Hence, the net rate of A production is shown in Eq. (13).

$$\frac{d[A]}{dt} = k_1 [Fe^{2+}][COD] - k_2 [A]^2 \quad (13)$$

The A is assumed that it is formed and spontaneously decomposed into  $A_2$ , so net rate of A production is equal to zero,  $\frac{d[A]}{dt} = 0$ .

$$0 = k_1 [Fe^{2+}][COD] - k_2 [A]^2$$

$$[A]^2 = \frac{k_1}{k_2} [Fe^{2+}][COD] \quad (14)$$

### 3.3. Net rate of $A_2$ production

Rate of  $A_2$  production from flocculation and entrapment is expressed by:

$$\frac{d[A_2]}{dt} = \frac{1}{2} k_2 [A]^2 + k_e [COD]$$

Rate of decrease in  $A_2$  to be sludge (sedimentation) is expressed by:

$$\frac{d[A_2]}{dt} = -k_{st} [A_2]$$

Hence, the net rate of  $A_2$  production is shown in Eq. (15).

$$\frac{d[A_2]}{dt} = \frac{1}{2} k_2 [A]^2 + k_e [COD] - k_{st} [A_2] \quad (15)$$

The  $A_2$  is also assumed that it is formed and spontaneously decomposed into sludge, so net rate of  $A_2$  production is equal to zero,  $\frac{d[A_2]}{dt} = 0$ .

$$0 = \frac{1}{2} k_2 [A]^2 + k_e [COD] - k_{st} [A_2]$$

$$[A_2] = \frac{\frac{1}{2} k_2 [A]^2 + k_e [COD]}{k_{st}} \quad (16)$$

### 3.4. Net rate of scum and sludge production

Rate of scum and sludge production is expressed by:

$$\frac{d[Sludge]}{dt} = k_{st} [A_2] - k_{sc} [Sludge] \quad (17)$$

$$\frac{d[Scum]}{dt} = k_{sc} [Sludge] \quad (18)$$

Substituting Eq. (14) and (16) to Eq. (17) to get Eq. (19)

$$\frac{d[Sludge]}{dt} = \frac{1}{2} k_2 [Fe^{2+}][COD] + k_e [COD] - k_{sc} [Sludge] \quad (19)$$

### 3.5. Net rate of decrease in COD through adsorption and entrapment

$$\frac{d[COD]}{dt} = -k_1 [Fe^{2+}][COD] - k_e [COD] \quad (20)$$

Therefore, the net rate for all components is shown in Table 2.

## 4. Methods

### 4.1. Vinasse

Vinasse was collected from PT. Madukismo located in Yogyakarta, Indonesia. It contained COD, total dissolved Fe and power of Hydrogen (pH) of  $100.16 \pm 0.29 \text{ g L}^{-1}$ ,  $38.79 \pm 0.09 \text{ mg L}^{-1}$  and  $4.35 \pm 0.05$  respectively.

### 4.2. Experimental set up

Beaker glass with volume of 1 L was used as EC batch reactor. Volume of vinasse treated in this study was 1 L. The iron plats with dimension of length, width and thickness of 20 cm, 3 cm and 3 mm were used as electrodes. The dimension of the plats immersed in vinasse was 9.5 cm, 3 cm and 3 mm (a 45° surface ( $A_s$ ) of  $28.5 \text{ cm}^2$ ). Therefore, the ratio of  $\frac{A_s}{V}$  was  $28.5 \text{ cm}^2 \text{ L}^{-1}$ . The distance of electrodes was 5.5 cm. Power DC supply (Long Wei, Series of LW-K3010D, 0–30 V, 0–10 A) was used as electrical current source. The agitation speed was maintained to be 200 rpm. Fig. 2 shows the experimental set up in this study.

### 4.3. Experimental design and procedures

Before used, the electrodes were soaked in HCl 5 %v/v solution for 15 min. After that, the electrodes were rinsed using distilled water and then weighted [25]. The initial pH of vinasse was varied to be  $4.35 \pm 0.05$ ,  $5.00 \pm 0.00$  and  $6.00 \pm 0.00$  by using NaOH (technical grade). Voltage was maintained on 10 V. The EC process was carried out for 60 min (3600 s) with duplicate of experiments (experiment a and b). During process, the current (I, Ampere) was recorded per 10 min (600 s). Since the  $A_s$  was assumed to be constant ( $28.5 \text{ cm}^2$ ), the current density ( $J$ , Ampere  $\text{cm}^{-2}$ ) was calculated with formula of  $I/28.5$ . The change of  $J$  during process was discussed in point of Results and Discussions. Every 600 s, the scum produced on the surface of vinasse was taken. Furthermore, 6 was dried under temperature of  $105–110 \text{ }^\circ\text{C}$  and weighted. Then, the pH was monitored using a digital pH meter (model ATC 2011) every 600 s. The solution temperature was measured by using a mercury thermometer. Furthermore, the solution sample was taken as much as 10–20 mL and then placed in reaction tube for settling as long as 24 h. After settling, 49 supernatants were taken for COD and total dissolved Fe analysis. The COD analysis was conducted through Open Reflux and Titration Method of SNI 06–6989.15-2004. The total dissolved Fe in solution was determined in Badan Tenaga Nuklir Nasional (BATAN) by using Atomic Absorption Spectroscopy (AAS). Before the analysis of dissolved Fe, the sample was filtered by using the Whatman 42. The measured total dissolved Fe was assumed that it represented the amount of  $Fe^{2+}$  ions in solution. After the EC process, the sacrificial electrode (anode) was rinsed using distilled water and weighted. The sludge mass produced during EC was calculated by using Eq. (21). Meanwhile, the conductivity of solution during process was determined using Eq. (22) [46].

$$\begin{aligned} \text{Sludge mass (t)} + \text{Scum mass (t)} &= \text{removed COD mass (t)} \\ &+ \text{removed total dissolved Fe mass (t)} \quad (21) \end{aligned}$$

**Table 2**  
Total mass balance for modeling.

Rate	Equation
$\frac{d[COD]}{dt}$	$-k_1 [Fe^{2+}][COD] - k_e [COD]$
$\frac{d[Fe^{2+}]}{dt}$	$\frac{J M_{Fe} A_s}{z F V} - k_1 [Fe^{2+}][COD]$
$\frac{d[Sludge]}{dt}$	$\frac{1}{2} k_2 [Fe^{2+}][COD] + k_e [COD] - k_{sc} [Sludge]$
$\frac{d[Scum]}{dt}$	$k_{sc} [Sludge]$

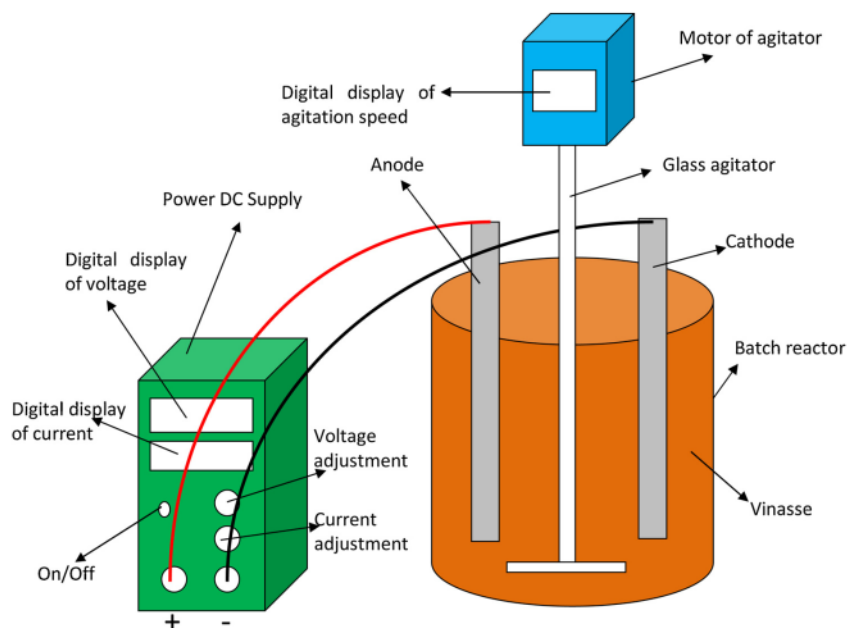


Fig. 2. Experimental set up.

**Table 3**  
Experimental data during EC process at variation of initial pH.

pH of 4.35 ± 0.05								
Time (second)	Current (A)	pH	Temperature (°C)	Scum (g L <sup>-1</sup> )	Weight loss of anode (g)	COD (g L <sup>-1</sup> )	Conductivity (μS cm <sup>-1</sup> )	Total dissolved Fe (mg L <sup>-1</sup> )
0	2.38 ± 0.00 <sup>a,b</sup>	4.35 ± 0.05 <sup>a,b</sup>	28.45 ± 0.45 <sup>a,b</sup>	0.00 ± 0.00 <sup>a,b</sup>	0.00 ± 0.00 <sup>a,b</sup>	100.16 ± 0.29 <sup>a,b</sup>	45833.33 ± 96.49 <sup>a,b</sup>	38.79 ± 0.09 <sup>b</sup>
600	2.52 ± 0.04 <sup>a,b</sup>	4.45 ± 0.05 <sup>a,b</sup>	30.75 ± 0.75 <sup>a,b</sup>	0.21 ± 0.18 <sup>a,b</sup>	Na	98.88 <sup>a</sup>	48631.58 ± 771.93 <sup>a,b</sup>	Na
1200	2.62 ± 0.04 <sup>a,b</sup>	4.50 ± 0.00 <sup>a,b</sup>	33.75 ± 0.75 <sup>a,b</sup>	0.37 ± 0.33 <sup>a,b</sup>	Na	97.65 ± 0.67 <sup>a,b</sup>	50561.40 ± 771.93 <sup>a,b</sup>	312.87 ± 3.93 <sup>b</sup>
1800	2.65 ± 0.10 <sup>a,b</sup>	4.60 ± 0.00 <sup>a,b</sup>	35.65 ± 1.15 <sup>a,b</sup>	0.56 ± 0.48 <sup>a,b</sup>	Na	96.95 ± 1.93 <sup>a,b</sup>	51140.35 ± 1929.82 <sup>a,b</sup>	Na
2400	2.68 ± 0.13 <sup>a,b</sup>	4.65 ± 0.05 <sup>a,b</sup>	37.90 ± 0.90 <sup>a,b</sup>	0.74 ± 0.62 <sup>a,b</sup>	Na	96.66 ± 2.22 <sup>a,b</sup>	51719.30 ± 2508.77 <sup>a,b</sup>	642.83 ± 8.59 <sup>b</sup>
3000	2.72 ± 0.12 <sup>a,b</sup>	4.80 ± 0.00 <sup>a,b</sup>	39.20 ± 1.20 <sup>a,b</sup>	0.83 ± 0.68 <sup>a,b</sup>	Na	96.87 ± 0.10 <sup>a,b</sup>	52394.74 ± 2219.30 <sup>a,b</sup>	Na
3600	2.72 ± 0.11 <sup>a,b</sup>	4.90 ± 0.00 <sup>a,b</sup>	40.45 ± 1.45 <sup>a,b</sup>	0.92 ± 0.74 <sup>a,b</sup>	-2.89 ± 0.02 <sup>a,b</sup>	95.33 ± 1.65 <sup>a,b</sup>	52491.23 ± 2122.81 <sup>a,b</sup>	1147.95 ± 2.02 <sup>b</sup>
pH of 5.00 ± 0.00								
Time (second)	Current (A)	pH	Temperature (°C)	Scum (g L <sup>-1</sup> )	Weight loss of anode (g)	COD (g L <sup>-1</sup> )	Conductivity (μS cm <sup>-1</sup> )	Total dissolved Fe (mg L <sup>-1</sup> )
0	2.66 ± 0.23 <sup>a,b</sup>	5.00 ± 0.00 <sup>a,b</sup>	29.00 ± 0.00 <sup>a,b</sup>	0.00 ± 0.00 <sup>a,b</sup>	0.00 ± 0.00 <sup>a,b</sup>	100.16 ± 0.29 <sup>a,b</sup>	51236.84 ± 4342.11 <sup>a,b</sup>	38.79 ± 0.09 <sup>b</sup>
600	2.80 ± 0.22 <sup>a,b</sup>	5.10 ± 0.10 <sup>a,b</sup>	32.00 ± 0.00 <sup>a,b</sup>	0.41 ± 0.19 <sup>a,b</sup>	Na	96.31 ± 1.09 <sup>a,b</sup>	54035.09 ± 4245.61 <sup>a,b</sup>	Na
1200	2.90 ± 0.28 <sup>a,b</sup>	5.20 ± 0.10 <sup>a,b</sup>	34.75 ± 0.25 <sup>a,b</sup>	0.80 ± 0.25 <sup>a,b</sup>	Na	93.79 ± 1.43 <sup>a,b</sup>	55868.42 ± 5307.02 <sup>a,b</sup>	296.26 ± 0.56 <sup>b</sup>
1800	2.94 ± 0.29 <sup>a,b</sup>	5.30 ± 0.10 <sup>a,b</sup>	36.90 ± 0.10 <sup>a,b</sup>	1.29 ± 0.54 <sup>a,b</sup>	Na	92.86 ± 0.50 <sup>a,b</sup>	56640.35 ± 5500.00 <sup>a,b</sup>	Na
2400	2.94 ± 0.29 <sup>a,b</sup>	5.45 ± 0.15 <sup>a,b</sup>	38.75 ± 0.25 <sup>a,b</sup>	2.08 ± 1.11 <sup>a,b</sup>	Na	92.63 ± 0.27 <sup>a,b</sup>	56640.35 ± 5500.00 <sup>a,b</sup>	631.86 ± 2.83 <sup>b</sup>
3000	2.91 ± 0.26 <sup>a,b</sup>	5.60 ± 0.20 <sup>a,b</sup>	40.00 ± 0.00 <sup>a,b</sup>	3.19 ± 1.76 <sup>a,b</sup>	Na	91.79 ± 1.11 <sup>a,b</sup>	56061.40 ± 4921.05 <sup>a,b</sup>	Na
3600	2.85 ± 0.26 <sup>a,b</sup>	5.85 ± 0.25 <sup>a,b</sup>	41.25 ± 0.25 <sup>a,b</sup>	4.54 ± 2.15 <sup>a,b</sup>	-3.00 ± 0.19 <sup>a,b</sup>	91.56 ± 0.88 <sup>a,b</sup>	54903.51 ± 4921.05 <sup>a,b</sup>	1018.80 ± 2.03 <sup>b</sup>
pH of 6.00 ± 0.00								
Time (second)	Current (A)	pH	Temperature (°C)	Scum (g L <sup>-1</sup> )	Weight loss of anode (g)	COD (g L <sup>-1</sup> )	Conductivity (μS cm <sup>-1</sup> )	Total dissolved Fe (mg L <sup>-1</sup> )
0	2.98 ± 0.18 <sup>a,b</sup>	6.00 ± 0.00 <sup>a,b</sup>	29.75 ± 0.75 <sup>a,b</sup>	0.00 ± 0.00 <sup>a,b</sup>	0.00 ± 0.00 <sup>a,b</sup>	100.16 ± 0.29 <sup>a,b</sup>	57412.28 ± 3377.19 <sup>a,b</sup>	38.79 ± 0.09 <sup>b</sup>
600	2.91 ± 0.28 <sup>a,b</sup>	6.15 ± 0.05 <sup>a,b</sup>	33.00 ± 1.00 <sup>a,b</sup>	1.59 ± 0.72 <sup>a,b</sup>	Na	96.19 <sup>a</sup>	56157.89 ± 5403.51 <sup>a,b</sup>	Na
1200	2.81 ± 0.34 <sup>a,b</sup>	6.55 ± 0.05 <sup>a,b</sup>	35.55 ± 0.55 <sup>a,b</sup>	3.55 ± 0.98 <sup>a,b</sup>	Na	91.46 <sup>a</sup>	54228.07 ± 6561.40 <sup>a,b</sup>	229.50 ± 3.24 <sup>b</sup>
1800	2.76 ± 0.41 <sup>a,b</sup>	7.05 ± 0.25 <sup>a,b</sup>	37.25 ± 1.25 <sup>a,b</sup>	5.41 ± 1.04 <sup>a,b</sup>	Na	91.46 <sup>a</sup>	53166.67 ± 7815.79 <sup>a,b</sup>	Na
2400	2.62 ± 0.44 <sup>a,b</sup>	7.25 ± 0.35 <sup>a,b</sup>	38.50 ± 1.50 <sup>a,b</sup>	7.19 ± 1.26 <sup>a,b</sup>	Na	90.71 <sup>a</sup>	50561.40 ± 8491.23 <sup>a,b</sup>	546.36 ± 0.83 <sup>b</sup>
3000	2.32 ± 0.37 <sup>a,b</sup>	7.40 ± 0.30 <sup>a,b</sup>	39.50 ± 1.50 <sup>a,b</sup>	9.09 ± 1.52 <sup>a,b</sup>	Na	88.46 ± 3.00 <sup>a</sup>	44771.93 ± 7140.35 <sup>a,b</sup>	Na
3600	2.02 ± 0.25 <sup>a,b</sup>	7.50 ± 0.20 <sup>a,b</sup>	40.00 ± 2.00 <sup>a,b</sup>	10.92 ± 1.89 <sup>a,b</sup>	-2.83 ± 0.44 <sup>a,b</sup>	86.21 ± 2.25 <sup>a</sup>	38885.96 ± 4921.05 <sup>a,b</sup>	864.09 ± 0.46 <sup>b</sup>

Remarks: Na, not analyzed; superscript a = data obtained from experiment a; superscript b = data obtained from experiment b; superscript a,b = data obtained from experiment a,b.

$$\kappa = \frac{Id}{VA_s} 10^6 \quad (22)$$

#### 4.4. Kinetic analysis

In this study, the measured data obtained during EC process were COD, total dissolved Fe in solution, scum and sludge. Furthermore, the data was used to build a mechanistic model. Furthermore, the error was calculated by using Eq. (23).

$$\text{Error} = \sum_{i=1}^n \left( \frac{\text{measured data} - \text{predicted data}}{\text{measured data}} \right)^2 \quad (23)$$

#### 4.5. Operating cost

The operating cost is an important term in EC process. According to Ozonar and Karagozlu [47], the operating cost consisted of energy, electrode, and chemical cost. Hence, calculation of operating cost (IDR L<sup>-1</sup>) was expressed in Eq. (24).

$$\frac{d[\text{Operating Cost}]}{dt} = a \frac{d[EnC]}{dt} + b \frac{d[EIC]}{dt} + c ChC \quad (24)$$

Unit prices of  $a$ ,  $b$  and  $c$  are as follows prices of electrical energy, electrode materials and chemicals. The electrical energy price for middle scale industrial use was estimated as 1115 IDR kWh<sup>-1</sup> (kilowatt hour) or  $30.97 \times 10^{-5}$  IDR Ws<sup>-1</sup> (watt second). The iron material price was estimated as 20,000 IDR kg<sup>-1</sup> or 20 IDR g<sup>-1</sup>. The chemical price for technical grade NaOH (flake) was estimated as 16,000 IDR kg<sup>-1</sup>. The  $EnC$  (Energy Consumption) and  $EIC$  (Electrode Consumption) were calculated using Eq. (25) [48] and Eq. (26) [49] respectively.

$$\frac{d[EnC]}{dt} = \frac{VI}{v} \quad (25)$$

$$\frac{d[EIC]}{dt} = \frac{JM_w A_s}{zFv} \quad (26)$$

### 5. Results and discussions

#### 5.1. Current density profile during EC

The current was monitored and presented in Table 3. Furthermore, the current density ( $J$ , Ampere cm<sup>-2</sup>) was calculated with formula of  $I/A_s$  in which the  $A_s$  was assumed to be constant (28.5 cm<sup>2</sup>). The change of  $J$  during process was shown in Fig. 3. In this study, the voltage was maintained to be constant (10 V). Thus, the change of current density was caused by the change of solution conductivity in which the higher the conductivity caused the higher the current density. The solution conductivity was also shown in Table 3.

Electrodissolution of Fe<sup>2+</sup> increased the conductivity. Meanwhile when the coagulants adsorbed the pollutants and they were removed by sedimentation or filtration, the conductivity of solution decreased. At initial pH of 4.35, the current density increased slowly from beginning to the end of process. That means, the electrodisolution rate of Fe<sup>2+</sup> and removal rate of COD were slow but the latter was slower. At initial pH of 5.00, current density increased from beginning until second 1800, after that it decreased. At range of second 0–1800, the electrodisolution rate of Fe<sup>2+</sup> was higher than removal rate of COD. Meanwhile at range of second 1800–3600, the electrodisolution rate of Fe<sup>2+</sup> was lower than removal rate of COD. At initial pH of 6.00, current density decreased until the end of process. Thus, commonly, the electrodisolution rate of Fe<sup>2+</sup> was lower than removal rate of COD at initial pH of 6.00. During EC process, the solution temperature changed because of the current supplied to the solution and electrolysis time [50]. The temperature profile was same for all variables (Table 3) in which initial temperature of 28.45–29.75 °C was to be final temperature of

40.00–41.25 °C.

#### 5.2. Comparison between measured and predicted electrode consumption

During EC process, the anode (Fe) is oxidized to Fe<sup>2+</sup> ion. The  $z$  can be 2 (Fe<sup>2+</sup>, ferrous) or 3 (Fe<sup>3+</sup>, ferric). Some authors believed that the Fe<sup>2+</sup> is produced from electrolysis of anode [51,52], however the others believed that Fe<sup>3+</sup> ion is produced directly during EC [53,54]. The value of  $z$  is important to be determined because it is directly connected to the proposed mechanistic model and operating cost calculation.

To find the appropriate  $z$  value, the electrode (anode) consumption during EC was predicted by using Eq. (26) with  $z = 2$  and  $z = 3$ . Furthermore, the predicted electrode consumption was compared with the measured data. Comparison between measured and predicted electrode consumption is shown in Fig. 4. Based on the Fig. 4, the calculation using  $z = 2$  gave much better prediction than  $z = 3$ . That means electrodisolution of anode in this study resulted Fe<sup>2+</sup> ion. Thus,  $z = 2$  was used in the mechanistic model and operating cost calculation. Lakshmanan et al. [43] also reported the same conclusion that Fe<sup>2+</sup> was generated at iron anode during EC, not Fe<sup>3+</sup>. The Fe<sup>3+</sup> ion might be formatted from oxidation of Fe<sup>2+</sup> because of the presence of dissolved oxygen and increasing in pH [43]. Therefore, Eq. (1) to (5) could be accepted.

#### 5.3. pH, COD and total dissolved Fe profile during EC

The profile of pH and COD during EC process is shown in Table 3. During the process, the H<sub>2</sub>O was reduced to be OH<sup>-</sup> ion and H<sub>2</sub> gas. Accumulation of OH<sup>-</sup> increased the pH of solution. For initial pH of 4.35 ± 0.05, 5.00 ± 0.00, 6.00 ± 0.00, the final pH was to be 4.90 ± 0.00, 5.85 ± 0.25, 7.50 ± 0.20 respectively. The pH level influences the iron species in solution. The higher the pH level, the more the dose of main coagulants of Fe(OH)<sub>2</sub> and Fe(OH)<sub>3</sub> presenting in the solution. At initial pH of 4.35, solution pH changed in range 4.35–4.90 during process. At that range, iron was in form of Fe<sup>2+</sup>, Fe(OH)<sub>2</sub>, Fe(OH)<sub>2</sub><sup>+</sup> and Fe(OH)<sub>3</sub> [37]. The Fe(OH)<sub>2</sub> and Fe(OH)<sub>3</sub> was coagulants responding in COD removal. The value of COD removal at initial pH of 4.35 was very low (4.83 %) because the main coagulant presenting in low concentration.

For initial pH of 5.00, the pH increased from 5.00 to 5.85. At that range, the amount of Fe<sup>2+</sup> decreased, while the amount of Fe(OH)<sub>2</sub><sup>+</sup>, Fe(OH)<sub>3</sub> and Fe(OH)<sub>2</sub> increased [37]. As consequence, the COD removal at initial pH of 5.00 ± 0.00 higher (8.59 %) than that at initial pH of 4.35 ± 0.05 (4.83 %). The highest COD removal (13.93 %) was obtained at initial pH of 6.00 ± 0.00. At that variable, pH increased from 6.00 to 7.50, so the amount of Fe<sup>2+</sup> ion decreased and the main coagulants of Fe(OH)<sub>3</sub> and Fe(OH)<sub>2</sub> were dominant in the solution [37]. The coagulants adsorbed the pollutants easily

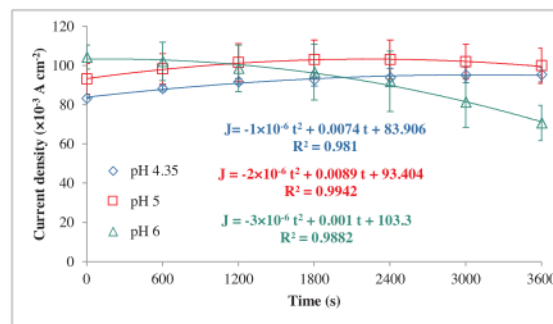


Fig. 3. Current density profile at variation of initial pH during EC.

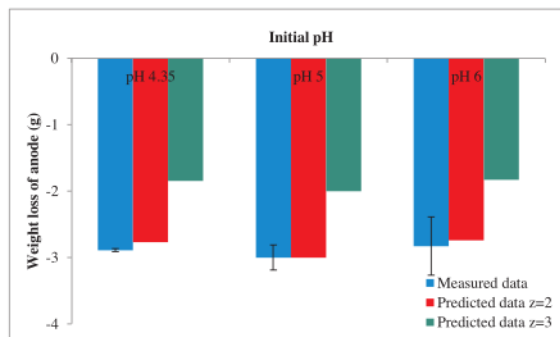


Fig. 4. Weight loss of anode after EC for 3600 s.

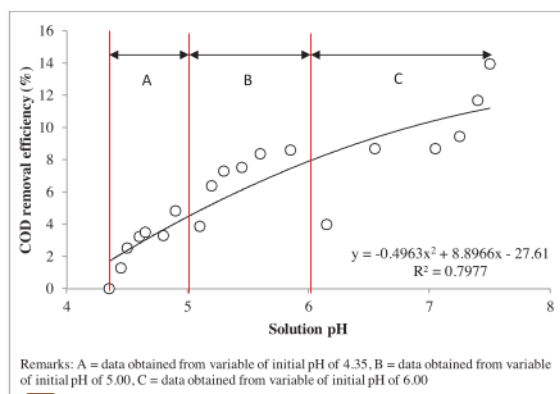


Fig. 5. The mechanism of solution pH on the COD removal efficiency.

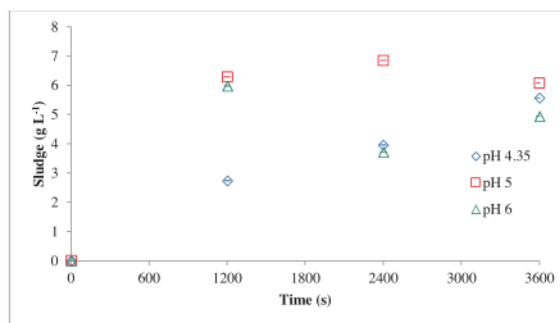


Fig. 6. Sludge production at variation of initial pH during EC.

so the COD removal was higher than the others. Demirbas and Kobya [30] also reported the same results with this study. For Fe electrode, increasing initial pH from 3 to 7 could increase COD removal from 60 to 90 %. At neutral pH, gelatinous metal coagulant was released in large amount in solution [25,55].

During EC process, solution pH changed. Thus, correlation between the mechanism of pH and COD removal efficiency was interesting to be studied. The COD removal efficiency was calculated by Eq. (27). The correlation is shown in Fig. 5.

$$\text{COD removal efficiency}(t)(\%) = \frac{\text{initial COD} - \text{COD}(t)}{\text{initial COD}} \times 100\% \quad (27)$$

Based on Fig. 5, increase in solution pH caused increase in COD removal efficiency. It had correlation with iron species in solution. The

higher the solution pH, the more the coagulants ( $\text{Fe}(\text{OH})_2$  and  $\text{Fe}(\text{OH})_3$ ) were formed [37]. Then, they adsorbed the pollutant so the COD removal efficiency was obtained in higher solution pH. However, the COD removal efficiency will decrease when the solution pH more than 8.00 [30,42]. In this study, initial pH of 6.00 showed the good phenomena of pH change where it changed from 6.00 to 7.50. The pH range was good for formation of coagulants. If initial pH of neutral is conducted, the solution pH range might be from 7.00 to more than 8.00. That range is still good for formation of the coagulants so initial pH of 7.00 will give the same result of COD removal efficiency with initial pH of 6.00. Furthermore, if initial pH of alkaline (pH of 8.00–14.00) is conducted, the COD removal efficiency decreases because the main coagulants will be dissolved again to be species of  $\text{Fe}(\text{OH})^+$ ,  $\text{Fe}(\text{OH})_3^-$  and  $\text{Fe}(\text{OH})_4^-$ . pH level affected the form of Fe species in solution. Coagulants ( $\text{Fe}(\text{OH})_3$  and  $\text{Fe}(\text{OH})_2$ ) were assumed to be sludge and scum completely. Furthermore, the  $\text{Fe}^{3+}$  ion that might be formed because of oxidation and hydrolysis of  $\text{Fe}^{2+}$  was completely become  $\text{Fe}(\text{OH})_3$ . Hence,  $\text{Fe}^{2+}$  remained dominantly in solution. In assumption, the remaining total dissolved Fe concentration measured by AAS was equal to the remaining  $\text{Fe}^{2+}$  concentration in solution. The remaining total dissolved Fe in solution is measured and shown in Table 3.

As explanation above, the higher the pH level, the more the  $\text{Fe}^{2+}$  ion was to be coagulants; consequently the more the COD was removed. There is good correlation between COD and total dissolved Fe profile during EC where the higher the remaining COD level, the higher the remaining total dissolved Fe. Based on Table 3, anode weight was decreased as much as  $-2.89 \pm 0.02$ ,  $-3.00 \pm 0.19$  and  $-2.83 \pm 0.44$  g for initial pH of 4.35, 5.00 and 6.00 respectively. After EC for 3600 s, the remaining total dissolved Fe at initial pH of 4.35, 5.00 and 6.00 was  $1147.95 \pm 2.02$ ,  $1018.80 \pm 2.03$  and  $864.09 \pm 0.46$  mg L<sup>-1</sup> respectively (Table 3). In other words, the removed total dissolved Fe in solution, which became coagulants adsorbing pollutants to form sludge and scum, at initial pH of 6.00 ( $2004.70$  mg L<sup>-1</sup> or 69.88 %) was higher than that at initial pH of 4.35 ( $1780.84$  mg L<sup>-1</sup> or 60.80 %) and pH 5.00 ( $2019.99$  mg L<sup>-1</sup> or 66.47 %).

Alkalinity could be measured by Eq. (28) [56]. In this study, pH of raw vinasse was 4.35. The NaOH was added to adjust pH of vinasse to be 5.00 and 6.00. During EC process, the  $\text{OH}^-$  ion was produced by reduction at cathode. Hence, in this study, the alkalinity change in vinasse mainly depended on  $\text{OH}^-$  concentration. Therefore, Eq. (28) was rearranged to be Eq. (29). The  $\text{OH}^-$  concentration was predicted by  $\exp(\text{pH} - 14)$ .

$$\text{Alkalinity} = [\text{HCO}_3^-] + 2[\text{CO}_3^{2-}] + [\text{OH}^-] - [\text{H}^+] \quad (28)$$

$$\text{Alkalinity} = [\text{OH}^-] \quad (29)$$

During EC process, the pH of vinasse increased (see Table 3). It showed the alkalinity of vinasse increased where the higher the pH of vinasse, the higher the alkalinity of vinasse would be. The  $\text{Fe}^{2+}$  ion, that was produced by oxidation at anode, consumed the OH to form coagulant of  $\text{Fe}(\text{OH})_2$ . Hence, the higher  $\text{OH}^-$  concentration, the more  $\text{Fe}(\text{OH})_2$  produced would be. Therefore, initial pH of 6 resulted more  $\text{Fe}(\text{OH})_2$  amount than the ones of the two others with lower initial pH.

#### 5.4. Scum and sludge profile during EC

The pollutants adsorbed by coagulants either go to base as sludge or go to surface as scum due to evolved  $\text{H}_2$ . The scum production during EC is presented in Table 3. The production rate of scum at initial pH of 6.00 was higher than that at initial pH of 4.35 and 5.00. Initial pH of 6 produced more coagulants than the others, so aggregates were easy to be formed. Furthermore, the aggregates were to be the bigger due to the



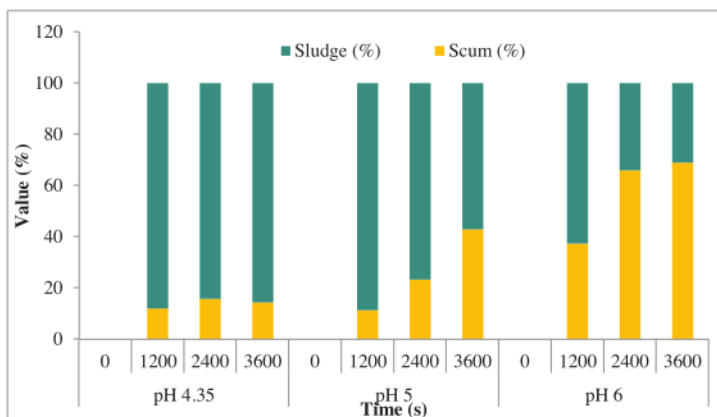


Fig. 7. Percentage of sludge and scum during EC process at various initial pH.

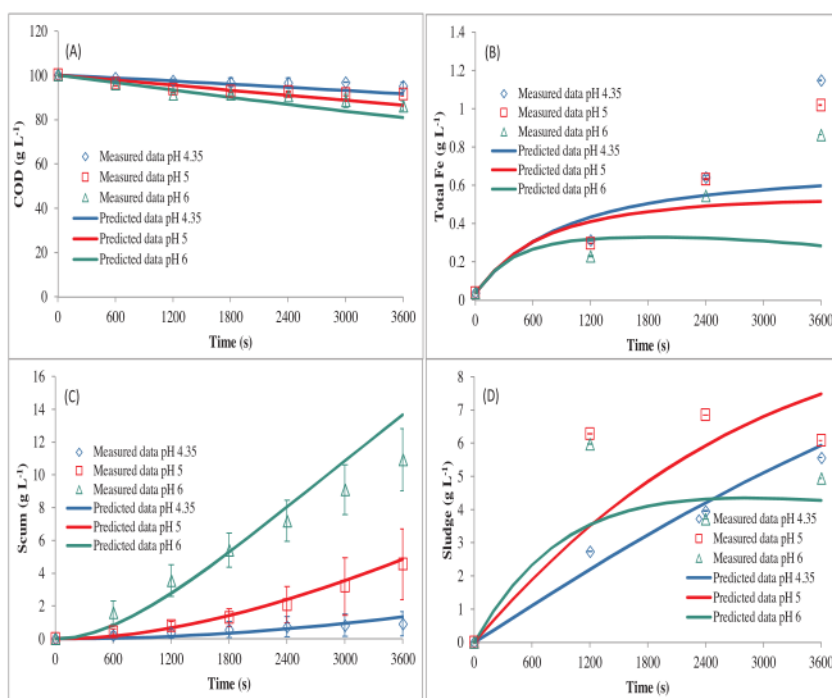


Fig. 8. Plotting between measured and predicted data using the mechanistic model (A) COD concentration, (B) total dissolved Fe concentration, (C) scum concentration, (D) sludge concentration.

Table 4

Kinetic constants obtained from simulation for EC process at various initial pH with ratio of  $A_e/v = 28.5 \text{ cm}^2 \text{ L}^{-1}$ , working volume of 1 L and electrode distance of 5.5 cm.

Kinetic constants	Initial pH		
	4.35	5.00	6.00
$k_1 \text{ (L g}^{-1} \text{ sec}^{-1}\text{)}$	$1.42 \times 10^{-5}$	$1.83 \times 10^{-5}$	$2.65 \times 10^{-5}$
$k_{sc} \text{ (sec}^{-1}\text{)}$	$1.19 \times 10^{-4}$	$3.02 \times 10^{-4}$	$1.10 \times 10^{-3}$
$k_d \text{ (sec}^{-1}\text{)}$	$1.79 \times 10^{-5}$	$3.30 \times 10^{-5}$	$5.14 \times 10^{-5}$
Error	1.8442	1.1271	1.3696

flocculation. Because of its big size, they were easy to go to surface as scum.

The sludge during EC was predicted by using Eq. (21) and then shown in Fig. 6. Furthermore, Fig. 7 showed the how much (%) the aggregates separated by sedimentation or by flotation. Commonly, the %sludge decreased and %scum increased during EC for all variation of initial pH. The solution pH increased during EC (Table 3). The higher the pH, the more the coagula were formed. The coagulants adsorbed the pollutants. In conclusion, the longer the electrolysis time, the more and the bigger the aggregates in solution. Because of the big size (or the large contact area), the aggregates are easier to be separated by flotation. After EC for 3600 s, the %scum on initial pH of 4.35, 5.00 and 6.00 was 14.23, 42.78 and 68.86 % respectively. It showed that initial pH of

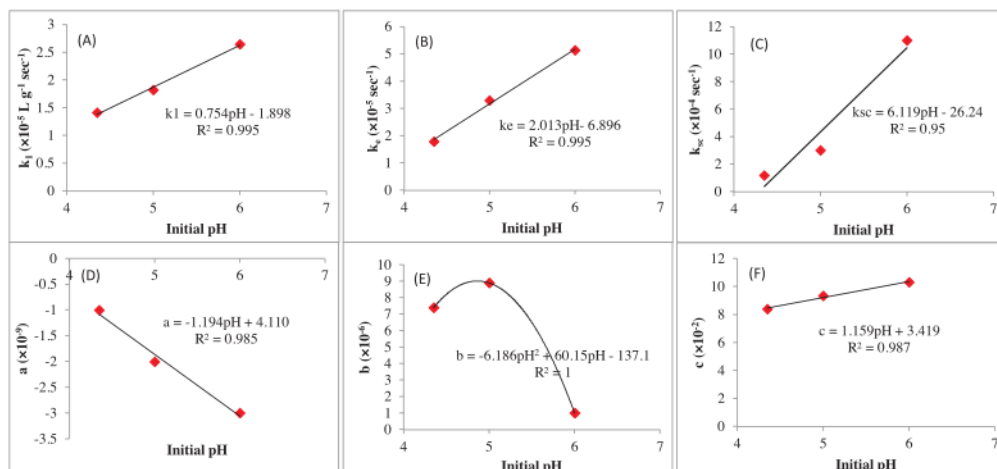


Fig. 9. Correlation between initial pH and kinetic constants of (A)  $k_1$ , (B)  $k_e$ , (C)  $k_{sc}$ , (D)  $a$ , (E)  $b$ , (F)  $c$ .

Table 5  
Operational cost EC process after 3600 s.

Initial pH	Electrode cost (IDR L <sup>-1</sup> )	Energy cost (IDR L <sup>-1</sup> )	Chemical cost (IDR L <sup>-1</sup> )	Total cost (IDR L <sup>-1</sup> )	Removed COD (g L <sup>-1</sup> )	Removed COD/Total cost (g IDR <sup>-1</sup> )
4.35	55.32	29.52	0	84.84	4.83	0.0570
5.00	60.01	32.02	77.95	169.98	8.60	0.0506
6.00	54.83	29.26	135.29	219.39	13.95	0.0636

6.00 produced more big aggregates than the others.

### 5.5. Modeling

The mechanistic model was successfully applied in this study. Plotting between measured and predicted data is shown in Fig. 8 and the kinetic constant values are presented in Table 4. The value of  $k_1$  represented the reaction rate constant of adsorption of pollutants (COD) on coagulants. The  $k_1$  value of initial pH of 6.00 ( $2.65 \times 10^{-5} \text{ L g}^{-1} \text{ sec}^{-1}$ ) was higher than the others ( $1.42 \times 10^{-5}$  and  $1.83 \times 10^{-5} \text{ L g}^{-1} \text{ sec}^{-1}$ ). As explanation above, initial pH of 6.00 resulted more coagulants than initial pH of 4.35 and 5.00, so the adsorption rate was faster.

Furthermore, the  $k_e$  value at initial pH of 6.00 was also higher than the others (Table 4). Kinetic constant of  $k_e$  represented the rate of entrapment when the bigger aggregate was formed. Thus, the more the aggregate in system, the easier the big aggregate was formed, so the easier the pollutant was entrapped. The rate of entrapment of pollutants at initial pH of 6.00 was the fastest because it produced the most coagulants of all variables.

Increasing initial pH from 4.35 to 6.00 increased the  $k_{sc}$  value. That phenomena showed that the higher the pH condition, the more the pollutants would be removed through flotation. Scum were easily produced at initial pH of 6 because aggregates were easy to be formed.

### 5.6. Development of mathematical equations to predict the EC performance in the other initial pH

The NaOH (technical grade) was added to adjust initial pH of vinasse to be 5.00 and 6.00 from the origin pH of 4.35. The addition of NaOH caused the increasing of electrolyte in vinasse. Hence, the initial current density was difference for all initial pH although the voltage was kept constant in 10 V. Current density profile during EC is shown in Fig. 3. The profile was figured through polynomial with degree of 2 with common formula  $J = at^2 + bt + c$ . The constant value of  $a$ ,  $b$  and  $c$  is shown in Fig. 3. Hence, it is important to predict correlation between

initial pH with value of  $a$ ,  $b$  and  $c$ . After that, the profile of current density during EC for other initial pH with range 4.35–6.00 can be predicted. The plotting between constants of  $a$ ,  $b$ ,  $c$  and initial pH is presented in Fig. 9. The EC process in this study was influenced by initial pH. Furthermore, the mathematical equation expressing the correlation between initial pH on kinetic constants of  $k_1$ ,  $k_{sc}$ ,  $k_e$  was built (see Fig. 9). By using equations in Fig. 9, EC performance with another initial pH with range 4.35–6.00 could be predicted.

### 5.7. Operating cost

Operating cost in EC process mainly depends on electrode, energy and chemical cost. Electrode cost was predicted successfully and shown in Table 5. Variable of initial pH of 5.00 needed higher electrode cost than initial pH of 4.35 and 6.00. The higher the current in EC, the more the electrode was to be  $\text{Fe}^{2+}$  ion in solution, so that the more the weight of electrode was needed. As consequence, the electrode cost was high. The high current in EC process also resulted the high energy cost. Furthermore, the chemical cost for all variables depended on using of NaOH for adjusting initial pH. The chemical cost for initial pH of 4.35, 5.00, 6.00 is shown in Table 5. Therefore, the total operating cost for initial pH of 4.35, 5.00 and 6.00 was 84.84, 169.98 and 219.39 IDR L<sup>-1</sup> respectively. Ratio between removed COD to total cost after 3600 s for initial pH of 4.35, 5.00 and 6.00 was 0.0570, 0.0506 and 0.0636 g IDR<sup>-1</sup> respectively (Table 5). Hence, initial pH of 6.00 was more effective and efficient to remove pollutants than initial pH of 4.35 and 5.00.

### 5.8. Comparison this study with other studies on COD removal

Comparison this study with other studies on COD removal is shown in Table 6. The COD removal efficiency in this study (13.90 %) was lower than that in study of Khandegar and Saroha [57], Asaithambi et al. [58], Aziz et al. [59], Asaithambi et al. [28] with value of 62–92.5 %. The difference was caused by that this study used very high initial

**Table 6**  
Comparison results in this study with others.

No	Wastes	Country	COD, (mg L <sup>-1</sup> )	Electrodes	Electrode distance (cm)	Current density (A m <sup>-2</sup> )	Temperature	Initial pH	Agitation speed (rpm)	Chemical addition	Operation time (min)	Removal efficiency (%)	References
1	Vinasse	Indonesia	100,160	irons	5.5	922.56 (average)	Room temperature	6	200	-	60	13.93	This study
2	Vinasse	Turkey	4,750	irons	0.3	200	Ambient temperature	5,15	-	0.2 M Na <sub>2</sub> SO <sub>4</sub>	180	14.3	[26]
3	Vinasse	India	3,360	irons	3	718	-	7.5	500	-	120	88	[57]
4	Vinasse	India	2,500	irons	1	300	Constant temperature = 30 ± 2 °C	6	-	-	240	62	[58]
5	Vinasse	Malaysia	2,000	irons	2	50	Room temperature	6	-	-	240	92.5	[59]
6	Vinasse	Malaysia	2,500	irons	3	13	Constant temperature = 35 ± 1 °C	7	100	234 mg/L H <sub>2</sub> O <sub>2</sub>	240	72	[28]

Remarks: COD<sub>i</sub>, initial COD in experiment.

COD concentration (103,180 mg L<sup>-1</sup>) and short operation time (60 min), while the others used low initial COD concentration (2,000–3,360 mg L<sup>-1</sup>) and long operation time (120–240 min). That was in line with report of Fayad [46] where removal efficiency decreases with the increase in initial pollutant concentration. Furthermore, according to Garcia-Segura et al. [37], the longer the operation time, the more the pollutants can be removed from the wastes. In other side, like this study, study of Yavuz [26] showed the low COD removal efficiency (14.3 %) although Yavuz [26] used low initial COD concentration 4,750 mg L<sup>-1</sup> and long operation time of 180 min. It might be caused by that the electrode distance was too close (0.3 cm). Very close of electrode distance is not good because the movement of ions is very quick so that will prevent the formation of flocs which are required to adsorb the pollutants [27].

## 6. Conclusion

Initial pH of 4.35, 5.00, 6.00 showed the difference of EC performance on COD, total dissolved Fe, scum, sludge and pH profile during process. The COD removal at initial pH of 6.00 (13.93 %) was higher than that at the others (4.83–8.59 %). The remaining total dissolved Fe at initial pH of 6.00 was lower than the others. Scum and sludge production increased with increasing initial pH from 4.35 to 6.00. Furthermore, a mechanistic model was successfully built and applied in EC for vinasse waste. In the model, reactions in EC were assumed that they were adsorption, flocculation, entrapment, flotation and sedimentation. Reaction rate constants of  $k_1$  (adsorption),  $k_{sc}$  (flotation) and  $k_e$  (entrapment) increased with increasing of initial pH from 4.35 to 6.00. Mathematical equations presenting correlation between initial pH with kinetic constants were successfully built. In operating cost calculation, ratio between removed COD to total operating cost for initial pH of 4.35, 5.00 and 6.00 was 0.0570, 0.0506 and 0.0636 g IDR<sup>-1</sup> respectively.

## CRedit authorship contribution statement

**Iqbal Syaichurrozi**: Conceptualization, Methodology, Software, Formal analysis, Investigation, Resources, Data curation, Writing - original draft, Visualization, Funding acquisition. **Sarto Sarto**: Conceptualization, Methodology, Resources, Writing - review & editing, Supervision, Project administration, Funding acquisition. **Wahyudi Budi Sediawan**: Methodology, Software, Validation, Writing - review & editing, Supervision. **Muslikhin Hidayat**: Software, Validation, Writing - review & editing, Supervision.

## Declaration of Competing Interest

The authors declare that they have no known competing financial interests or personal relationships that could have appeared to influence the work reported in this paper.

## Acknowledgement

The authors thank to Lembaga Pengelola Dana Pendidikan (LPDP), Kementerian Keuangan, Republik Indonesia via Beasiswa Unggulan Dosen Indonesia-Dalam Negeri (BUDI-DN) scholarship for financial support.

## References

- [1] D. Khataiwada, S. Silveira, Scenarios for bioethanol production in Indonesia: How we meet mandatory blending targets? Energy 119 (2017) 351–361, <https://doi.org/10.1016/j.energy.2016.12.073>.
- [2] I. Syaichurrozi, S. Suhirman, T. Hidayat, Effect of initial pH on anaerobic co-digestion of *Salvinia molesta* and rice straw for biogas production and kinetics, Biocatal. Agric. Biotechnol. 16 (2018) 594–603, <https://doi.org/10.1016/j.bcab.2018.10.007>.



- [3] I. Syaichurrozi Budiyo, S. Sumardiono, Predicting kinetic model of biogas production and biodegradability organic materials: Biogas production from vinasse at variation of COD/N ratio, *Bioresour. Technol.* 149 (2013) 390–397, <https://doi.org/10.1016/j.biortech.2013.09.088>.
- [4] J.A. Siles, I. García-García, A. Martín, M.A. Martín, Integrated ozonation and bi-methanization treatments of vinasse derived from ethanol manufacturing, *J. Hazard. Mater.* 188 (2011) 247–253, <https://doi.org/10.1016/j.jhazmat.2011.01.096>.
- [5] V.G. de Barros, R.M. Duda, J. da Silva Vantini, W.P. Omori, M.I.T. Ferro, R.A. de Oliveira, Improved methane production from sugarcane vinasse with filter cake in thermophilic UASB reactors, with predominance of Methanothermobacter and Methanosarcina archaea and Thermotoga bacteria, *Bioresour. Technol.* 244 (2017) 371–381, <https://doi.org/10.1016/j.biortech.2017.07.106>.
- [6] K. Lutoslawki, A. Ryznar-Luty, E. Cibis, M. Krzywonos, T. Miskiewicz, Biodegradation of beet molasses vinasse by a mixed culture of microorganisms: Effect of aeration conditions and pH control, *J. Environ. Sci. China (China)* 23 (11) (2011) 1823–1830, [https://doi.org/10.1016/S1001-0742\(10\)60579-7](https://doi.org/10.1016/S1001-0742(10)60579-7).
- [7] I. Budiyo, S. Syaichurrozi, Sumardiono, Effect of total solid content to biogas production rate from vinasse, *Int. J. Eng. 27 (2)* (2014) 177–184, <https://doi.org/10.5829/idosi.ije.2014.27.02b.02>.
- [8] A. Sepehri, M.-H. Sarrafzadeh, Effect of nitrifiers community on fouling mitigation and nitrification efficiency in a membrane bioreactor, *Chem Eng Process: Process Intensification* 128 (2018) 10–18, <https://doi.org/10.1016/j.jcep.2018.04.006>.
- [9] A. Sepehri, M.-H. Sarrafzadeh, M. Avateffazeli, Interaction between *Chlorella vulgaris* and nitrifying-enriched activated sludge in the treatment of wastewater with low C/N ratio, *J. Clean. Prod.* 247 (2019) 119164, <https://doi.org/10.1016/j.jclepro.2019.119164>.
- [10] X. Zhang, Q. Huang, F. Deng, H. Huang, Q. Wan, M. Liu, Y. Wei, Mussel-inspired fabrication of functional materials and their environmental applications: progress and prospects, *Appl. Mater. Today*. 7 (2017) 222–238, <https://doi.org/10.1016/j.apmt.2017.04.001>.
- [11] G. Zeng, L. Huang, Q. Huang, M. Liu, D. Xu, H. Huang, Z. Yang, F. Deng, X. Zhang, Y. Wei, Rapid synthesis of MoS<sub>2</sub>-PDA-Ag nanocomposites as heterogeneous catalysts and antimicrobial agents via microwave irradiation, *Appl. Surf. Sci.* 459 (2018) 588–595, <https://doi.org/10.1016/j.apsusc.2018.07.144>.
- [12] Y. Liu, K. Ai, L. Lu, Polydopamine and Its Derivative Materials: Synthesis and Promising Applications in Energy, Environmental, and Biomedical Fields, *Chem. Rev.* 114 (9) (2014) 5057–5115, <https://doi.org/10.1021/cr400407a>.
- [13] G. Zeng, T. Chen, L. Huang, M. Liu, R. Jiang, Q. Wan, Y. Dai, Y. Wen, X. Zhang, Y. Wei, Surface modification and drug delivery applications of MoS<sub>2</sub> nanosheets with polymers through the combination of mussel inspired chemistry and SET-LRP, *J. Taiwan. Inst. Chem. Eng.* 82 (2018) 205–213, <https://doi.org/10.1016/j.jtice.2017.08.025>.
- [14] Q. Huang, J. Zhao, M. Liu, Y. Li, J. Ruan, Q. Li, J. Tian, X. Zhu, X. Zhang, Y. Wei, Synthesis of polyacrylamide immobilized molybdenum disulfide (MoS<sub>2</sub>@PDA/PAM) composites via mussel-inspired chemistry and surface-initiated atom transfer radical polymerization for removal of copper (II) ions, *J. Taiwan. Inst. Chem. Eng.* 86 (2018) 174–184, <https://doi.org/10.1016/j.jtice.2017.12.027>.
- [15] G. Zeng, X. Liu, M. Liu, Q. Huang, D. Xu, Q. Wan, H. Huang, F. Deng, X. Zhang, Y. Wei, Facile preparation of carbon nanotubes based carboxymethyl chitosan nanocomposites through combination of mussel inspired chemistry and Michael addition reaction: characterization and improved Cu<sup>2+</sup> removal capability, *J. Taiwan. Inst. Chem. Eng.* 68 (2016) 446–454, <https://doi.org/10.1016/j.jtice.2016.09.008>.
- [16] X. Zhang, Q. Huang, M. Liu, J. Tian, G. Zeng, Z. Li, K. Wang, Q. Zhang, Q. Wan, F. Deng, Y. Wei, Preparation of amine functionalized carbon nanotubes via a bioinspired strategy and their application in Cu<sup>2+</sup> removal, *Appl. Surf. Sci.* 343 (2015) 19–27, <https://doi.org/10.1016/j.apsusc.2015.03.081>.
- [17] Q. Huang, M. Liu, L. Mao, D. Xu, G. Zeng, H. Huang, R. Jiang, F. Deng, X. Zhang, Y. Wei, Surface functionalized SiO<sub>2</sub> nanoparticles with cationic polymers via the combination of mussel inspired chemistry and surface initiated atom transfer radical polymerization: characterization and enhanced removal of organic dye, *J. Colloid Interface Sci.* 499 (2017) 170–179, <https://doi.org/10.1016/j.jcis.2017.03.102>.
- [18] Q. Huang, M. Liu, J. Chen, Q. Wan, J. Tian, L. Huang, R. Jiang, Y. Wen, X. Zhang, Y. Wei, Facile preparation of MoS<sub>2</sub> based polymer composites via mussel inspired chemistry and their high efficiency for removal of organic dyes, *Appl. Surf. Sci.* 419 (2017) 35–44, <https://doi.org/10.1016/j.apsusc.2017.05.006>.
- [19] Q. Huang, J. Zhao, M. Liu, J. Chen, X. Zhu, T. Wu, J. Tian, Y. Wen, X. Zhang, Y. Wei, Preparation of polyethylene polyamine@tannic acid encapsulated MgAl-layered double hydroxide for the efficient removal of copper (II) ions from aqueous solution, *J. Taiwan. Inst. Chem. Eng.* 82 (2018) 92–101, <https://doi.org/10.1016/j.jtice.2017.10.019>.
- [20] Y. Liu, H. Huang, D. Gan, L. Guo, M. Liu, J. Chen, F. Deng, N. Zhou, X. Zhang, Y. Wei, A facile strategy for preparation of magnetic graphene oxide composites and their potential for environmental adsorption, *Ceram. Int.* 44 (15) (2018) 18571–18577, <https://doi.org/10.1016/j.ceramint.2018.07.081>.
- [21] Q. Huang, M. Liu, J. Zhao, J. Chen, G. Zeng, H. Huang, J. Tian, Y. Wen, X. Zhang, Y. Wei, Facile preparation of polyethyleneimine-tannins coated SiO<sub>2</sub> hybrid materials for Cu<sup>2+</sup> removal, *Appl. Surf. Sci.* 427 (2018) 535–544, <https://doi.org/10.1016/j.apsusc.2017.08.233>.
- [22] D. Gan, M. Liu, H. Huang, J. Chen, J. Dou, Y. Wen, Q. Huang, Z. Yang, X. Zhang, Y. Wei, Facile preparation of functionalized carbon nanotubes with tannins through mussel-inspired chemistry and their application in removal of methylene blue, *J. Mol. Liq.* 271 (2018) 246–253, <https://doi.org/10.1016/j.molliq.2018.08.079>.
- [23] Y. Lei, Y. Cui, Q. Huang, J. Dou, D. Gan, F. Deng, M. Liu, X. Li, X. Zhang, Y. Wei, Facile preparation of sulfonic groups functionalized MXenes for efficient removal of methylene blue, *Ceram. Int.* 45 (2019) 17653–17661, <https://doi.org/10.1016/j.ceramint.2019.05.331>.
- [24] N. Kannan, G. Karthikeyan, N. Tamilselva, Comparison of treatment potential of electrocoagulation of distillery effluent with and without activated Area catechu nut carbon, *J. Hazard. Mater.* B137 (2006) 1803–1809, <https://doi.org/10.1016/j.jhazmat.2006.05.048>.
- [25] C. David, M. Arivazhagan, F. Tuvakara, Decolorization of distillery spent wash effluent by electrooxidation (EC and EF) and Fenton processes: a comparative study, *Ecotoxicol. Environ. Saf.* 121 (2015) 142–148, <https://doi.org/10.1016/j.ecoenv.2015.04.038>.
- [26] Y. Yavuz, EC and EF processes for the treatment of alcohol distillery wastewater, *Sep. Purif. Technol.* 53 (2007) 135–140, <https://doi.org/10.1016/j.seppur.2006.08.022>.
- [27] V. Khandegar, A.K. Saroha, Electrochemical treatment of distillery spent wash using aluminum and iron electrodes, *Chin. J. Chem. Eng.* 20 (3) (2012) 439–443, [https://doi.org/10.1016/S1004-9541\(11\)60204-8](https://doi.org/10.1016/S1004-9541(11)60204-8).
- [28] P. Asaithambi, Baharak Sajjadi, A. Aziz, A. Raman, W. Daud, W.M.A. Bin, Performance evaluation of hybrid electrocoagulation process parameters for the treatment of distillery industrial effluent, *Process Saf. Environ. Prot.* 104 (2016) 406–412, <https://doi.org/10.1016/j.psep.2016.09.023>.
- [29] J.A. Davila, F. Machuca, N. Marrianga, Treatment of vinasses by electrocoagulation–electroflotation using the Taguchi method, *Electrochim. Acta* 56 (2011) 7433–7436, <https://doi.org/10.1016/j.electacta.2011.07.015>.
- [30] E. Demirbas, M. Kobya, Operating cost and treatment of metalworking fluid wastewater by chemical coagulation and electrocoagulation processes, *Process Saf. Environ. Prot.* 105 (2017) 79–90, <https://doi.org/10.1016/j.psep.2016.10.013>.
- [31] M. Elazzouzi, Kh. Haboubi, M.S. Elyoubi, Electrocoagulation flocculation as a low-cost process for pollutants removal from urban wastewater, *Chem. Eng. Res. Des.* 117 (2017) 614–626, <https://doi.org/10.1016/j.cherd.2016.11.011>.
- [32] B.-Y. Tak, B.-S. Tak, Y.-J. Kim, Y.-J. Park, Y.-H. Yoon, G.-H. Min, Optimization of color and COD removal from livestock wastewater by electrocoagulation process: application of Box–Behnken design (BBD), *J. Ind. Eng. Chem.* 28 (2015) 307–315, <https://doi.org/10.1016/j.jiec.2015.03.008>.
- [33] D. Wagle, C.-J. Lin, T. Nawaz, H.J. Shipley, Evaluation and optimization of electrocoagulation for treating Kraft paper mill wastewater, *J. Environ. Chem. Eng.* 8 (1) (2020) 103595, <https://doi.org/10.1016/j.jece.2019.103595>.
- [34] E.K. Mroczek, D. Graham, L. Bacon, Removal of arsenic and silica from geothermal fluid by electrocoagulation, *J. Environ. Chem. Eng.* 7 (4) (2019) 103232, <https://doi.org/10.1016/j.jece.2019.103232>.
- [35] M. Kobya, P.I. Omwene, Z. Ukundimana, Treatment and operating cost analysis of metalworking wastewaters by a continuous electrocoagulation reactor, *J. Environ. Chem. Eng.* (2019), <https://doi.org/10.1016/j.jece.2019.103526>.
- [36] H.J. You, I.S. Han, Effects of dissolved ions and natural organic matter on electrocoagulation of As(III) in groundwater, *J. Environ. Chem. Eng.* 4 (1) (2016) 1008–1016, <https://doi.org/10.1016/j.jece.2015.12.034>.
- [37] S. Garcia-Segura, M.M.S.G. Eiband, J.V. de Melo, C.A. Martínez-Huitle, Electrocoagulation and advanced electrocoagulation processes: a general review about the fundamentals, emerging applications and its association with other technologies, *J. Electroanal. Chem. Lausanne (Lausanne)* 801 (2017) 267–299, <https://doi.org/10.1016/j.jelechem.2017.07.047>.
- [38] A. Mohammadi, A. Khadir, R.M.A. Tehrani, Optimization of nitrogen removal from an anaerobic digester effluent by electrocoagulation process, *J. Environ. Chem. Eng.* 7 (3) (2019) 103195, <https://doi.org/10.1016/j.jece.2019.103195>.
- [39] L. Largitte, R. Pasquier, A review of the kinetics adsorption models and their application to the adsorption of lead by an activated carbon, *Chem. Eng. Res. Des.* 109 (2016) 495–504, <https://doi.org/10.1016/j.cherd.2016.02.006>.
- [40] Y.A. Ouaisa, M. Chabani, A. Amrane, A. Bensmaili, Removal of tetracycline by electrocoagulation: kinetic and isotherm modeling through adsorption, *J. Environ. Chem. Eng.* 2 (1) (2014) 177–184, <https://doi.org/10.1016/j.jece.2013.12.009>.
- [41] A.G. Khorram, N. Fallah, Treatment of textile dyeing factory wastewater by electrocoagulation with low sludge settling time: optimization of operating parameters by RSM, *J. Environ. Chem. Eng.* 6 (1) (2018) 635–642, <https://doi.org/10.1016/j.jece.2017.12.054>.
- [42] M.E. Olya, A. Pirkarami, Electrocoagulation for the removal of phenol and aldehyde contaminants from resin effluent, *Water Sci. Technol.* 68 (9) (2013) 1940–1949, <https://doi.org/10.2166/wst.2013.439>.
- [43] D. Lakshmanan, D.A. Clifford, G. Samanta, Ferric Ion Generation During Iron Electrocoagulation, *Environ. Sci. Technol.* 43 (2009) 3853–3859, <https://doi.org/10.1021/es8036669>.
- [44] J.N. Hakizimana, B. Gourich, M. Chafi, Y. Stiriba, C. Vieal, P. Drogui, J. Naja, Electrocoagulation process in water treatment: a review of electrocoagulation modeling approaches, *Desalination* 404 (2017) 1–21, <https://doi.org/10.1016/j.desal.2016.10.011>.
- [45] M. Dolati, A.A. Aghapour, H. Khorsandi, S. Karimzade, Boron removal from aqueous solutions by electrocoagulation at low concentrations, *J. Environ. Chem. Eng.* 5 (5) (2017) 5150–5156, <https://doi.org/10.1016/j.jece.2017.09.055>.
- [46] N. Fayad, The Application of Electrocoagulation Process for Wastewater Treatment and for the Separation and Purification of Biological Media, *Chemical and Process Engineering, Université Clermont Auvergne, 2017 Doctoral Thesis*.
- [47] F. Ozyonar, B. Karagozlu, Treatment of pretreated coke wastewater by electrocoagulation and electrochemical peroxidation processes, *Sep. Purif. Technol.* 150 (2015) 268–277, <https://doi.org/10.1016/j.seppur.2015.07.011>.
- [48] H. Singh, B.K. Mishra, Assessment of kinetics behavior of electrocoagulation process for the removal of suspended solids and metals from synthetic water, *Int. J. Civ. Struct. Environ. Infrastruct. Eng. Res. Dev.* 22 (2) (2017) 141–148, <https://doi.org/>



- 10.4491/eer.2016.029.
- [49] M. Koby, F. Ozyonar, E. Demirbas, E. Sik, M.S. Oncel, Arsenic removal from groundwater of Sivas-Şarkışla Plain, Turkey by electrocoagulation process: comparing with iron plate and ball electrodes, *J. Environ. Chem. Eng.* 3 (2) (2015) 1096–1106, <https://doi.org/10.1016/j.jece.2015.04.014>.
- [50] S.O. Giwa, K. Polat, H. Hapoglu, The effects of operating parameters on temperature and electrode dissolution in electrocoagulation treatment of petrochemical wastewater, *Int. J. Eng. Res. Technol.* 1 (10) (2012) 1–9.
- [51] R. Parga, D.L. Cocke, V. Valverde, Characterization of electrocoagulation for removal of chromium and arsenic, *Chem. Eng. Technol.* 28 (5) (2005) 605–612, <https://doi.org/10.1002/ceat.200407035>.
- [52] M.Y. Mollah, R. Schennach, J.R. Parga, D.L. Cocke, Electrocoagulation (EC) - science and applications, *J. Hazard. Mater.* 84 (1) (2001) 29–41, [https://doi.org/10.1016/S0304-3894\(01\)00176-5](https://doi.org/10.1016/S0304-3894(01)00176-5).
- [53] M. Koby, E. Senturk, M. Bayramoglu, Treatment of poultry slaughterhouse wastewaters by electrocoagulation, *J. Hazard. Mater.* 133 (1) (2006) 172–176, <https://doi.org/10.1016/j.jhazmat.2005.10.007>.
- [54] M.Y. Mollah, P.G. Morkovsky, A.G. Gomes, M. Kesmez, J. Parga, Fundamentals, Present and Future Perspectives of Electrocoagulation, *J. Hazard. Mater.* 114 (1-3) (2004) 199–210, <https://doi.org/10.1016/j.jhazmat.2004.08.009>.
- [55] E. Nariyan, A. Aghababaei, M. Silanpää, Removal of pharmaceutical from water with an electrocoagulation process; effect of various parameters and studies of isotherm and kinetic, *Sep. Purif. Technol.* 188 (2017) 266–281, <https://doi.org/10.1016/j.seppur.2017.07.031>.
- [56] S.E. Manahan, *Water Chemistry: Green Science and Technology of Nature's Most Renewable Resource*, CRC Press, Taylor & Francis Group, 2010.
- [57] V. Khandegar, A.K. Saroha, Electrocoagulation of distillery spentwash for complete organic reduction, *Int. J. Chemtech Res.* 5 (2) (2013) 712–718.
- [58] P. Asaithambi, M. Susree, R. Saravanathamizhan, M. Matheswaran, Ozone assisted electrocoagulation for the treatment of distillery effluent, *Desalination* 297 (2012) 1–7, <https://doi.org/10.1016/j.desal.2012.04.011>.
- [59] A.R.A. Aziz, P. Asaithambi, W.M.A.B.W. Daud, Combination of electrocoagulation with advanced oxidation processes for the treatment of distillery industrial effluent, *Process Saf. Environ. Prot.* 99 (2016) 227–235, <https://doi.org/10.1016/j.psep.2015.11.010>.

# Mechanistic model of electrocoagulation process for treating vinasse waste: Effect of initial pH

## ORIGINALITY REPORT

9%

SIMILARITY INDEX

5%

INTERNET SOURCES

8%

PUBLICATIONS

%

STUDENT PAPERS

## PRIMARY SOURCES

- 1 Tuane Emerick, José L. Vieira, Marcos Henrique L. Silveira, Jair Juarez João. "Ultrasound-assisted electrocoagulation process applied to the treatment and reuse of swine slaughterhouse wastewater", *Journal of Environmental Chemical Engineering*, 2020  
Publication 1%
- 2 Xiaoyong Zhang, Qiang Huang, Fengjie Deng, Hongye Huang, Qing Wan, Meiyong Liu, Yen Wei. "Mussel-inspired fabrication of functional materials and their environmental applications: Progress and prospects", *Applied Materials Today*, 2017  
Publication 1%
- 3 [ir.xjtlu.edu.cn](http://ir.xjtlu.edu.cn)  
Internet Source <1%
- 4 [repository.udem.edu.co](http://repository.udem.edu.co)  
Internet Source <1%
- 5 Abdurrahman Akyol. "Treatment of paint manufacturing wastewater by

## electrocoagulation", Desalination, 2012

Publication

---

6	Zhen Lei, Li Zhi, Hongyu Jiang, Rong Chen, Xiaochang Wang, Yu-You Li. "Characterization of microbial evolution in high-solids methanogenic co-digestion of canned coffee processing wastewater and waste activated sludge by an anaerobic membrane bioreactor", Journal of Cleaner Production, 2019 Publication	<1 %
7	dokumen.pub Internet Source	<1 %
8	eprints.mdx.ac.uk Internet Source	<1 %
9	pure.rug.nl Internet Source	<1 %
10	untirta.ac.id Internet Source	<1 %
11	Marcela Marcondes de Santana, Everton Fernando Zanoelo, Cristina Benincá, Flavio Bentes Freire. "Electrochemical treatment of wastewater from a bakery industry: Experimental and modeling study", Process Safety and Environmental Protection, 2018 Publication	<1 %

---

12

P. Sakthisharmila, P.N. Palanisamy, P. Manikandan. "Removal of benzidine based textile dye using different metal hydroxides generated in situ electrochemical treatment-A comparative study", Journal of Cleaner Production, 2018

Publication

<1 %

13

[etd.aau.edu.et](http://etd.aau.edu.et)

Internet Source

<1 %

14

[jmrt.com.br](http://jmrt.com.br)

Internet Source

<1 %

15

Xiaokun Ye, Junya Zhang, Yan Zhang, Yuancai Lv, Rongni Dou, Shulong Wen, Lianghao Li, Yuancai Chen, YongYou Hu. "Treatment of Ni-EDTA containing wastewater by electrocoagulation using iron scraps packed-bed anode", Chemosphere, 2016

Publication

<1 %

16

[semarakilmu.com.my](http://semarakilmu.com.my)

Internet Source

<1 %

17

Hendra Hendra, Indra Setiawan, Hernadewita Hernadewita, Hermiyetti Hermiyetti. "Evaluation of Product Quality Improvement Against Waste in the Electronic Musical Instrument Industry", Jurnal Ilmiah Teknik Elektro Komputer dan Informatika, 2021

Publication

<1 %



18

Wan Sieng Yeo, Adhi Yuniarto. "The external mass transfer model for the hydrolysis of palm olein using immobilized lipase in a scaled-up recirculated packed-bed reactor", *Journal of Environmental Chemical Engineering*, 2019

Publication

&lt;1 %

19

Leila Abbasvash, Nasrin Shadjou. " Synthesize of cyclodextrin functionalized dendritic fibrous nanosilica and its application for the removal of organic dye (malachite green) ", *Journal of Molecular Recognition*, 2020

Publication

&lt;1 %

20

Sergi Garcia-Segura, Maria Maesia S.G. Eiband, Jailson Vieira de Melo, Carlos Alberto Martínez-Huitle. "Electrocoagulation and advanced electrocoagulation processes: A general review about the fundamentals, emerging applications and its association with other technologies", *Journal of Electroanalytical Chemistry*, 2017

Publication

&lt;1 %

21

[repositorio.unesp.br](https://repositorio.unesp.br)

Internet Source

&lt;1 %

22

Mouna Ghazouani, Latifa Bousselmi, Hanene Akrou. "Combined electrocoagulation and electrochemical treatment on BDD electrodes for simultaneous removal of nitrates and

&lt;1 %

phosphates", Journal of Environmental  
Chemical Engineering, 2020

Publication

---

23

Zohal Safaei Mahmoudabadi, Alimorad Rashidi, Davood Mohammady Maklavany. "Optimizing treatment of alcohol vinasse using a combination of advanced oxidation with porous  $\alpha$ -Fe<sub>2</sub>O<sub>3</sub> nanoparticles and coagulation-flocculation", Ecotoxicology and Environmental Safety, 2022

Publication

---

24

[kclpure.kcl.ac.uk](http://kclpure.kcl.ac.uk)

Internet Source

---

25

[link.springer.com](http://link.springer.com)

Internet Source

---

26

Abdulkarim Almukdad, MhdAmmar Hafiz, Ahmed T. Yasir, Radwan Alfahel, Alaa H. Hawari. "Unlocking the application potential of electrocoagulation process through hybrid processes", Journal of Water Process Engineering, 2021

Publication

---

27

Adedeji Adebukola Adelodun, Jane Catherine Ngila, Do-Gun Kim, Young-Min Jo. "Isotherm, Thermodynamic and Kinetic Studies of Selective CO<sub>2</sub> Adsorption on Chemically Modified Carbon Surfaces", Aerosol and Air Quality Research, 2016

<1 %

<1 %

<1 %

<1 %

<1 %

28

Dibya Ranjan Rout, Hara Mohan Jena. "Polyethylene glycol functionalized reduced graphene oxide coupled with zinc oxide composite adsorbent for removal of phenolic wastewater", Environmental Research, 2022

Publication

---

<1 %

29

Kadarkarai Govindan, Arumugam Angelin, Murali Rangarajan. "Critical evaluation of mechanism responsible for biomass abatement during electrochemical coagulation (EC) process: A critical review", Journal of Environmental Management, 2018

Publication

---

<1 %

30

Mohan Saravanan, Nurani Pabmanavhan Sambhamurthy, Meenatchisundaram Sivarajan. "Treatment of Acid Blue 113 Dye Solution Using Iron Electrocoagulation", CLEAN - Soil, Air, Water, 2010

Publication

---

<1 %

31

Sun, Meng, Fayuan Chen, Jiu-hui Qu, Huijuan Liu, and Ruiping Liu. "Optimization and control of Electro-Fenton process by pH inflection points: A case of treating acrylic fiber manufacturing wastewater", Chemical Engineering Journal, 2015.

Publication

---

<1 %

32

Fuat Özyonar, Ömür Gökkuş, Muhammed Sabuni. "Removal of disperse and reactive dyes from aqueous solutions using ultrasound-assisted electrocoagulation", *Chemosphere*, 2020

Publication

&lt;1 %

33

Heidmann, I.. "Removal of Cr(VI) from model wastewaters by electrocoagulation with Fe electrodes", *Separation and Purification Technology*, 20080606

Publication

&lt;1 %

34

Laleh Shamaei, Behnam Khorshidi, Basil Perdicakis, Mohtada Sadrzadeh. "Treatment of oil sands produced water using combined electrocoagulation and chemical coagulation techniques", *Science of The Total Environment*, 2018

Publication

&lt;1 %

35

M. Kobya, S. Delipinar. "Treatment of the baker's yeast wastewater by electrocoagulation", *Journal of Hazardous Materials*, 2008

Publication

&lt;1 %

36

Natthaphon Ardhan, Elvin J. Moore, Chantaraporn Phalakornkule. "Novel anode made of iron scrap for a reduced-cost electrocoagulator", *Chemical Engineering Journal*, 2014

&lt;1 %



37

Peipei Song, Qianqian Song, Zhaohui Yang, Guangming Zeng, Haiyin Xu, Xin Li, Weiping Xiong. "Numerical simulation and exploration of electrocoagulation process for arsenic and antimony removal: Electric field, flow field, and mass transfer studies", Journal of Environmental Management, 2018

Publication

---

<1 %

38

Qiang Huang, Meiyong Liu, Jiao Zhao, Junyu Chen et al. "Facile preparation of polyethylenimine-tannins coated SiO<sub>2</sub> hybrid materials for Cu<sup>2+</sup> removal", Applied Surface Science, 2017

Publication

---

<1 %

39

Runyu Xu, Zhinian Yang, Yunxia Niu, Duo Xu, Jia Wang, Jinlong Han, Hao Wang. "Removal of microplastics and attached heavy metals from secondary effluent of wastewater treatment plant using interpenetrating bipolar plate electrocoagulation", Separation and Purification Technology, 2022

Publication

---

<1 %

40

Yasaman Boroumand, Amir Razmjou, Parisa Moazzam, Fereshteh Mohagheghian et al. "Mussel inspired bacterial denitrification of water using fractal patterns of

<1 %

polydopamine", Journal of Water Process  
Engineering, 2020

Publication

41

[biointerfaceresearch.com](https://www.biointerfaceresearch.com)

Internet Source

<1 %

42

Abbas A. Al-Raad, Marlia M. Hanafiah.  
"Removal of inorganic pollutants using  
electrocoagulation technology: A review of  
emerging applications and mechanisms",  
Journal of Environmental Management, 2021

Publication

<1 %

43

Mohammad Dodangeh, Elmira Pajootan,  
Mehrdad Mohammadian, Norman S. Allen,  
Roya Eskandari Fard. "Alkali-clearing process  
optimization of the newly synthesized  
disperse dye and its promising removal from  
wastewater using electrocoagulation",  
Desalination and Water Treatment, 2014

Publication

<1 %

44

Neanderson Galvão, Jeanette Beber de Souza,  
Carlos Magno de Sousa Vidal. "Landfill  
leachate treatment by electrocoagulation:  
Effects of current density and electrolysis  
time", Journal of Environmental Chemical  
Engineering, 2020

Publication

<1 %

45

Shiv Kumar Verma, Vinita Khandegar, Anil. K.  
Saroja. "Removal of Chromium from

<1 %

Electroplating Industry Effluent Using Electrocoagulation", Journal of Hazardous, Toxic, and Radioactive Waste, 2013

Publication

46

[ebin.pub](http://ebin.pub)  
Internet Source

<1 %

47

[wlapwww.gov.bc.ca](http://wlapwww.gov.bc.ca)  
Internet Source

<1 %

48

[www.pub.iapchem.org](http://www.pub.iapchem.org)  
Internet Source

<1 %

49

Pankaj A. Shinde, Tejas M. Ukarde, Preeti H. Pandey, Hitesh S. Pawar. "Distillery spent wash: An emerging chemical pool for next generation sustainable distilleries", Journal of Water Process Engineering, 2020

Publication

<1 %

50

Syreina SAYEGH, Fida Tanos, Amr Nada, Geoffroy Lesage et al. "Tunable TiO<sub>2</sub>-BN-Pd nanofibers by combining electrospinning and Atomic Layer Deposition to enhance photodegradation of acetaminophen", Dalton Transactions, 2022

Publication

<1 %

51

A.K. Wardani, D. Ariono, S. Subagjo, IG. Wenten. "Fouling tendency of PDA/PVP surface modified PP membrane", Surfaces and Interfaces, 2020

Publication

<1 %

---

52

Chunjiang An, Gordon Huang, Yao Yao, Shan Zhao. "Emerging usage of electrocoagulation technology for oil removal from wastewater: A review", Science of The Total Environment, 2017

Publication

---

<1 %

53

Fuess, Lucas Tadeu, and Marcelo Loureiro Garcia. "Bioenergy from stillage anaerobic digestion to enhance the energy balance ratio of ethanol production", Journal of Environmental Management, 2015.

Publication

---

<1 %

54

Zakaria Al-Qodah, Mohammad Al-Shannag. "Heavy metal ions removal from wastewater using electrocoagulation processes: A comprehensive review", Separation Science and Technology, 2017

Publication

---

<1 %

---

Exclude quotes      On

Exclude matches      Off

Exclude bibliography      On



# Mechanistic model of electrocoagulation process for treating vinasse waste: Effect of initial pH

---

GRADEMARK REPORT

---

FINAL GRADE

**/0**

GENERAL COMMENTS

**Instructor**

---

PAGE 1

---

PAGE 2

---

PAGE 3

---

PAGE 4

---

PAGE 5

---

PAGE 6

---

PAGE 7

---

PAGE 8

---

PAGE 9

---

PAGE 10

---

PAGE 11

---

PAGE 12

---